Influence of Amorphous Alkaline Lignin on the Crystallization Behavior and Thermal Properties of Bacterial Polyester

Wang Shichao, Xiang Hengxue, Wang Renlin, Zhou Zhe, Zhu Meifang

State Key Laboratory for Modification of Chemical Fibers and Polymer Materials, College of Materials Science and Engineering, Donghua University, Shanghai 201620, China
Correspondence to: Z. Meifang (E‑mail: zhumf@dhu.edu.cn)

ABSTRACT: Bacterial polyester poly(3-hydroxybutyrate-co-3-hydroxyvalerate) (PHBV) and alkaline lignin composites were prepared via melt processing method, and the influence of amorphous lignin on the crystallization behavior and thermal properties of PHBV were investigated. It was found that dual melting peaks appeared in DSC curves of PHBV/lignin composites, while only one single peak existed in PHBV. The non-isothermal crystallization process analyzed by Jeziorny method suggested that lignin changed the nucleation mode of composites and hindered the crystallization rate of PHBV. Data calculated from the results of WAXD demonstrated that lignin did not change the basic crystal structure of PHBV, but decreased the average size of the lamellar stacks. POM results confirmed that the effect of lignin on the crystallization behavior of PHBV carried out in two opposite way, namely the enhanced effect of nucleation and the hindered effect of growth. Besides, the thermal stability of composites was also decreased significantly. © 2014 Wiley Periodicals, Inc. J. Appl. Polym. Sci. **2015**, *132*, 41325.

INTRODUCTION

Due to the environmental pollution and the shortage of petroleum resources, the design of polymer and composites has been focused on the field based on renewable natural resources. Several biodegradable polymers have been developed from renewable substances in the past decades. Among these polymers, bacterial polyester polyhydroxyalkanoates (PHAs) have received a great deal of interest owing to the fact that they are full biodegradable and biosynthetic polymers.[1] The earliest discovered and most extensively studied polymer in PHAs' family is poly(3-hydroxybutyrate) (PHB). However, the application of PHB is relatively limited due to its brittleness and low degradation rate caused by its high crystallinity (>90%). To solve this problem, 3-hydroxyvalerate (HV) unit is introduced into PHB chains to form PHBV via fermentation.[2] The properties of PHBV are related to the ratio of HV in PHBV. Normally, it is hard to synthesis PHBV with high HV content by microorganisms. Besides, PHBV is found to have a very low degree of heterogeneous nucleation density due to the high purity, leading to the formation of large spherulites with circular breaks around the center and cracks in the radial direction of the spherulites.[3,4] Therefore, the application of commercial available PHBV is hindered by the high cost, as well as the high brittleness caused by low nucleation density and large spherulites.

Numerous efforts have been made to change this situation. Among them, the incorporation of other functional additives into the polymer matrix to form composites has received more and more attention, especially the incorporation of micro/nanoparticles. The effects of micro/nanoparticles on the crystallization and mechanical behaviors of composites have been investigated extensively, including the inorganic particles[5–8] and organic particles.[9–12] In recent years, an increasing interest has been given to the preparation and property studies of full biodegradable composites containing micro/nanoparticles. Ten et al. studied the thermal and mechanical properties of PHBV/cellulose nanowhiskers (CNW) composites and found that CNW was an effective nucleation agent for PHBV.[9] Tensile strength, Young's modulus and toughness of PHBV were increased with the increasing concentration of CNW. The authors also suggested that the improvement of mechanical properties of PHBV could be attributed to the strong interactions between PHBV and CNW phases. Nattaporn *et al* further studied the interactions between OH groups in cellulose acetate butyrate and C=O groups in PHB.[13]

In our previous work, we found that amorphous thermoplastic polyurethane destroyed the integrity of PHBV spherulites, which was good for the improvement of toughness.[14] Based on the above evidences, we suppose that amorphous micro/

nanoparticles with some interactional groups could enhance the nucleation density of PHBV and destroy the integrity of PHBV spherulites at the same time. The ideal candidate of amorphous micro/nanoparticles is lignin powder. Together with cellulose and hemicellulose, lignin is one of the main constituents of wood.[15] It is generally obtained as a byproduct in the paper production. As a low-density, low-abrasive and low-cost material, lignin shows a fascinating prospect to replace the inorganic fillers in the use of filler.[16,17]

To the best of our knowledge, very little work has been reported about the composites of PHBV/lignin and the interactions between them, needless to say the effects of alkaline lignin on the crystallization behavior and thermal properties of PHBV.[18,19] In this study, we prepared PHBV/lignin composites with different lignin contents from 1 wt % to 10 wt % by melt blending. The crystallization behavior, basic crystal structure and the interactions between PHBV and lignin were intensively studied. We hope that this study will give a clue on the influence of the amorphous alkaline lignin on the crystallization behavior and thermal properties of the bacterial polyester.

EXPERIMENTAL

Materials
Commercial PHBV ($Mw = 2.67 \times 10^5$, HV = 1.09 mol %) was kindly supplied by Ningbo Tianan Biologic Material Co., Ltd (Ningbo, China). Alkaline lignin was purchased from TCI (Shanghai, China). The content of methoxyl group and ignition residue of alkaline lignin was 10.0–12.0% and 20.0–29.0%, respectively. All materials were used as received without further purification.

Sample Preparation
PHBV powders and alkaline lignin powders were dried under vacuum for 24 h at 80°C prior to melt processing to get rid of moisture. The melt blending process was carried out in a Haake Rheocord 90 batch mixer equipped with a pair of roller-type blades. The contents of lignin were 1, 3, 5, and 10% of the total weight, respectively. The roller speed and temperature were maintained at 40 rpm and 165°C, and the process time was 4 min. The neat PHBV sample was also processed under the same condition for comparison. All samples were dried under vacuum for 24 h at 80°C before testing.

Measurements and Characterization
Differential Scanning Calorimetry. DSC analysis was performed on DSC instrument (TA Instruments, Q20) to determine the melting and crystallization behaviors of PHBV/lignin composites. Samples with weight of about 8 mg were first heated to 190°C and kept isothermal for 2 min at 190°C to eliminate the thermal history of composites, then cooled down to −50°C and reheated to 190°C. The heating rate was 10°C/min, and the cooling rate were 2.5°C/min, 5°C/min, 10°C/min, 20°C/min, and 40°C/min, respectively.

Wide Angle X-ray Diffraction. WAXD experiments were performed on a Rigaku d/Max-2550 PC X-ray diffractometer to determine the crystal parameters and crystallinity of composites. Diffraction patterns were recorded at room temperature with

Table I. The Calculated Crystallinity and DSC Thermal Data of PHBV/Lignin Composites

PHBV/Lignin	T_{m1} (°C)	T_{m2} (°C)	ΔH_f (J g^{-1})	X_c (%)	T_p (°C)
100/0	170.7	–	89.4	61.0	92.9
99/1	171.5	173.5	92.6	63.8	87.5
97/3	164.1	171.4	91.3	64.2	90.2
95/5	154.2	165.7	89.9	64.6	83.1
90/10	144.4	158.4	85.6	64.9	76.9

the 2θ range of 5–60° and scanning rate of 2°/min. The wavelength (λ) of irradiation source was 1.541 Å.

Polarizing Optical Microscopy. Spherulites morphology of PHBV/lignin composites was observed using a polarizing optical microscope (POM) (DM2500P) equipped with a temperature controller. Each sample was sandwiched between two thin glass sides, kept at 190°C for 2 min on hot stage, and then cooled down to 85°C at a rate of 100°C/min. The growth of spherulites as a function of time was recorded by taking photographs at constant time intervals.

Thermogravimetric Analysis. TGA was performed on Netzsch (TG 209 F1 Iris) thermogravimetric analyzer to study the thermal stability of PHBV/lignin composites. Samples with the weight of 5–10 mg were heated from 30°C to 600°C with a heating rate of 10°C/min under a continuous nitrogen flow of 30 mL/min.

RESULTS AND DISCUSSION

Melting and Crystallization Behavior of PHBV/Lignin Composites
DSC test was used to study the influence of amorphous alkaline lignin on the melting behavior and crystallization process of PHBV, and the thermal data are listed in Table I. Thermograms of the second melting behavior are illustrated in Figure 1. Only one single melting peak was observed in neat PHBV matrix. However, dual melting peaks appeared in PHBV/lignin composites when lignin was incorporated. It was noted that the low-temperature peak (T_{m1}) was the main peak for pure PHBV, while the area of high-temperature peak (T_{m2}) became larger with increasing amount of lignin in the PHBV/lignin composites. This can be explained that T_{m1} is probably related to the homogeneous nucleation of PHBV, while T_{m2} is probably related to the heterogeneous nucleation of PHBV. Because of the nucleation effect of lignin powder, much more crystalline nuclei were produced in the PHBV/lignin composites compared with that in PHBV. Therefore, the high-temperature melting peak became larger, while the low-temperature peak was suppressed with the addition of lignin. Similar phenomenon has been observed in PHBV/organophilic montmorillonite nanocomposites.[20]

The non-isothermal crystallization behavior of PHBV/lignin composites is shown in Figure 2. It was found that the crystallization peak temperatures T_p showed a decrease trend with the addition of lignin, suggesting that the addition of lignin affected
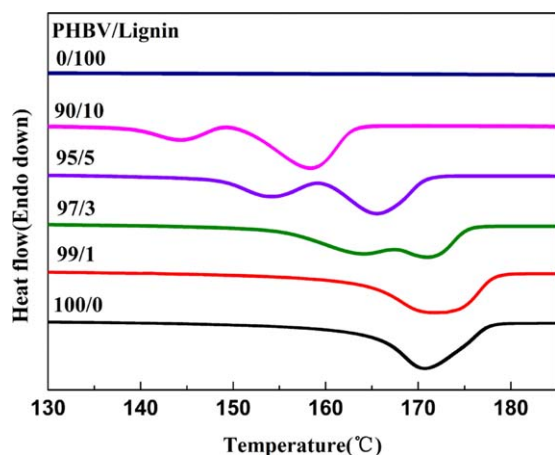
Figure 1. The melting behavior of PHBV/lignin composites. [Color figure can be viewed in the online issue, which is available at wileyonlinelibrary.com.]

Figure 2. The cooling crystallization behavior of PHBV/lignin composites. [Color figure can be viewed in the online issue, which is available at wileyonlinelibrary.com.]

the crystallization process of PHBV. The crystallization process of PHBV was influenced by lignin powder in two opposite ways. On one hand, the lignin powder acted as a kind of nucleating agent in PHBV matrix, which increased the nucleation density, as well as the crystallization process of composites. On the other hand, the existence of lignin restricted the motion of PHBV chains owing to the hydrogen bonding interactions between the hydroxyl groups in lignin and ester groups in PHBV.[21] Thus, the crystallization temperature would decrease when the effect of interactions was greater than that of nucleation. In addition, both the melting and crystallization peaks of PHBV/lignin composites were wider than that of PHBV, indicating that the crystal size distribution in PHBV/lignin composites was broader than that in PHBV.[22] Besides, the degree of crystallinity (X_c) was also calculated by following equation to examine the changes caused by the addition of lignin:[23]

$$X_c = \frac{\Delta H_f}{\left(1 - \omega_{\text{Lignin}}\right)\Delta H_f^0} \times 100\% \qquad (1)$$

where X_c is the degree of crystallinity for PHBV and its composites, ω_{Lignin} is the weight fraction of lignin, ΔH_f is the measured heat of melting and ΔH_f^0 is the heat of fusion of 100% crystalline PHBV. Considering the low HV content in PHBV in our study, ΔH_f^0 is chosen as 146.6 J g^{-1} for PHB.[24] The calculated crystallinity is also listed in Table I. It was found that the crystallinity of PHBV/lignin composites was increased with the addition of lignin powder, suggesting an enhanced nucleation effect of lignin powder.

To further investigate the effect of lignin on the crystallization behavior of PHBV, the non-isothermal crystallization kinetics of PHBV and its composites were analyzed by using Jeziorny method to give more detailed information.[25] Jeziorny method is a modified Avrami equation, which is applied to the non-isothermal crystallization process. In this method, data are analyzed by treating non-isothermal crystallization process as isothermal crystallization process, and then revised by corresponding parameters. The revised equation can be described as follows:

$$1 - X_t = \exp(-Z_t \cdot t^n) \text{ or } \lg\{-\ln[1 - X_t]\} = n\lg t + \lg Z_t \qquad (2)$$
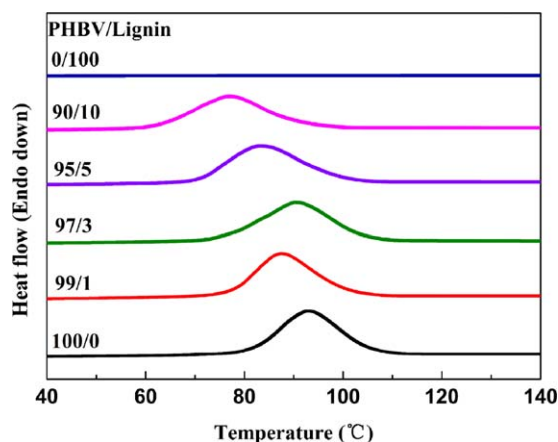
where t is the crystallization time, X_t is the relative degree of crystallinity, which is determined by means of the following equation:[26]

$$X_t = \int_0^t \left(\frac{dH}{dt}\right) dt \Big/ \int_0^\infty \left(\frac{dH}{dt}\right) dt \qquad (3)$$

n is the Avrami exponent, Z_t is the rate constant during the non-isothermal crystallization process. Taking the cooling rate (Q) into consideration, Z_c is introduced to reflect more accurate rate constant. It can be expressed as follows:

$$\lg Z_c = (\lg Z_t)/Q \qquad (4)$$

The parameters n and Z_c depend on the nucleation mechanism and growth geometry of composites. The plots of X_t versus t for PHBV and PHBV/3% lignin composites at different cooling rates are shown in Figure 3(a,b), respectively. The initial crystallization temperature (T_i), crystallization peak temperature (T_p), crystallization enthalpy (ΔH_c), as well as the half-time of crystallization ($t_{1/2}$) defined as the time required to attain half of the final crystallinity are listed in Table II. It was found that T_i, T_p, ΔH_c and $t_{1/2}$ were decreased with the increase of cooling rate for both PHBV and PHBV/3% lignin composites. In lower cooling rate, PHBV molecular chains have enough time for crystallization, and the crystal size is relatively big, leading to the higher T_i, T_p, ΔH_c and a longer $t_{1/2}$. Compared with PHBV at different cooling rate, the T_i, T_p, and ΔH_c of PHBV/3% lignin composites showed a decreased trend while the $t_{1/2}$ showed an increased trend with the addition of lignin. This phenomenon can be explained that when lignin was added to PHBV, the motion of PHBV chains were restricted due to the hydrogen bonding interactions between PHBV and lignin,[21] leading to the delay of crystallization process. Besides, the appearance of lignin destroyed the integrity of PHBV crystals as well as decreased the size of PHBV crystal.

Figure 4(a,b) are the double logarithmic plots of the Avrami analysis based on eq. (2) for PHBV and PHBV/3% lignin composites, respectively. At early crystallization process, both the curves of PHBV and PHBV/3% lignin composites were
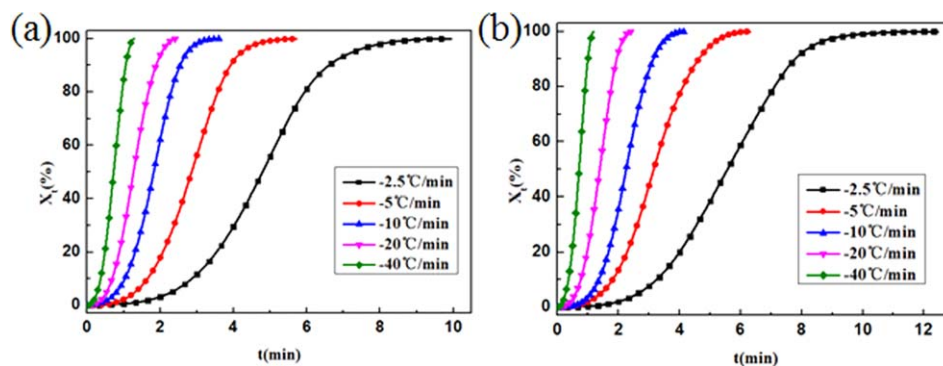
Figure 3. X_t as a function of t for PHBV (a) and PHBV/3% lignin composite (b). [Color figure can be viewed in the online issue, which is available at wileyonlinelibrary.com.]

presented favorable linear relationship. Avrami exponent n values and crystallization rate constant Z_c values can be obtained from the slope and intercept of these linear curves in this stage. As described in Table II, the Avrami exponent n of PHBV and its composites were kept around 3. In general, $n = 3$ corresponds to two kinds of possible crystallization mechanisms, namely the three-dimensional growth combined with heterogeneous nucleation and the two-dimensional growth combined with homogeneous nucleation.[26] It is generally accepted that PHBV melts are inclined to undergo homogeneous nucleation.[27] Therefore, the crystallization mode of PHBV might correspond to the two-dimensional growth. Similar conclusion that the spherulites' growth does not completely follow the spherulitic propagation has been reported elsewhere.[28] In PHBV/3% lignin composites, lignin powder provided many nucleating sites, and the nucleation occurred on the surface of lignin. As a result, the crystallization mode of PHBV changed to the three-dimensional spherulitic growth grounded on lignin nuclei.[29] Thus, although the values of n were almost the same for PHBV and its composites, the crystallization mechanisms were quite different. Moreover, the values of calculated Z_c for PHBV/3% lignin showed a decreased trend compared with these of PHBV at different cooling rate, which further confirmed the hindered effect of lignin on the crystallization rate of PHBV. From Figure 4(a,b), we can also find that the Avrami curves turned out to be nonlinear at later crystallization process, which was mainly caused by the impinging of PHBV spherulites.

Crystal Structure of PHBV/Lignin Composites

It has been reported that PHBV exhibits an unusual phenomenon of isodimorphism and it crystallizes in PHB unit cell when the content of HV is lower than 30 mol %.[30,31] From WAXD patterns of PHBV/lignin composites shown in Figure 5, we can see clearly that only characteristic diffraction peaks of PHB type lattice existed in both PHBV and its composites, indicating that the basic crystal structure of PHBV was not changed by the incorporation of lignin. The d-spacing (d_{hkl}) of the (020), (110), and (002) diffractions, as well as the average size of the lamellar stacks (H_{hkl}) perpendicular to the (020), (110), and (002) lattice planes were calculated by Bragg's equation and Scherrer formula. According to the Bragg's equation:[32]

$$d_{hkl} = \frac{\lambda}{2 \sin \theta_{hkl}} \tag{5}$$

where θ is the X-ray diffraction angle and λ is the wavelength. The calculated results are given in Table III. No obvious change was observed among the d-space of PHBV and its composites, suggesting that the parameters of PHBV unit cell were not influenced by the addition of lignin. The average size of the lamellar stacks was determined by the Scherrer formula.

$$H_{hkl} = \frac{K\lambda}{\beta_{hkl} \cos \theta_{hkl}} = \frac{K\lambda}{F_{WHM} \cdot \frac{\pi}{180} \cdot \cos \theta_{hkl}} \tag{6}$$

where K is the constant and the value is 0.89, β_{hkl} is the integral breadth or breadth at half-maximum intensity, F_{WHM} is the

Table II. Kinetics Parameters of PHBV and PHBV/3% Lignin Composite During Nonisothermal Crystallization Process

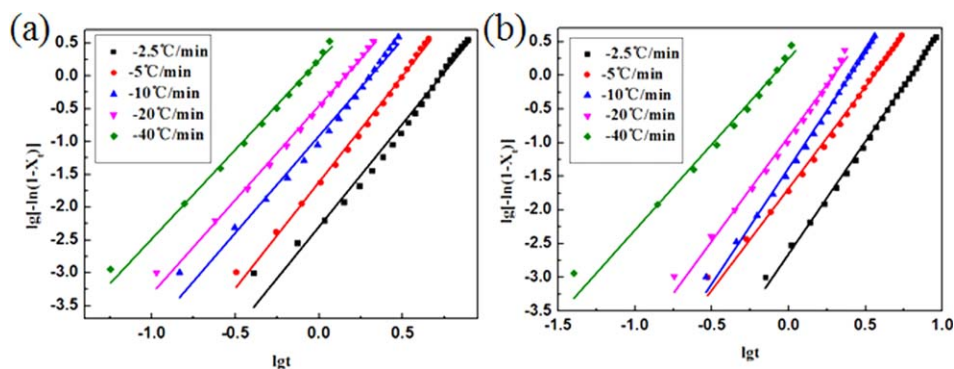| Samples	Q (°C min⁻¹)	n	Z_c	$t_{1/2}$ (min)	T_i (°C)	T_p (°C)	ΔH_c (J g⁻¹)
PHBV	2.5	3.14	0.12	4.79	122.45	109.62	86.55
	5	3.23	0.36	2.86	118.36	103.14	76.58
	10	2.95	0.81	1.83	112.80	92.94	65.30
	20	2.86	0.95	1.27	106.19	80.90	51.76
	40	2.72	1.02	0.73	98.93	68.98	26.20
PHBV/3% lignin	2.5	3.35	0.09	5.57	117.11	103.17	79.23
	5	3.02	0.46	3.16	112.56	96.83	76.31
	10	3.43	0.73	2.25	110.93	90.28	65.85
	20	3.11	0.90	1.39	100.28	70.41	47.47
	40	2.55	1.02	0.75	91.48	60.92	15.63

Figure 4. Plots of lg{-ln[1-X_{t}]} vs lgt for PHBV (a) and PHBV/3% lignin composite (b). [Color figure can be viewed in the online issue, which is available at wileyonlinelibrary.com.]

half-diffraction peak width.[31] As can be seen from Table III, the size of lamellar stacks decreased slightly after lignin was added. As we discussed earlier, hydrogen bonding interactions were formed between ─OH groups in lignin particles and C═O groups in PHBV matrix. During the crystallization process, lignin particles disturbed the regularity of PHBV molecular chains and further decreased the PHBV crystallite size of the lamellar stacks. Similar result has been reported in PHBV/zinc oxide nanoparticles system.[8] In addition, the crystallinity of composites can also be obtained from X-ray diffraction intensity data by dividing the area of crystalline peaks by the total area of crystalline peaks and amorphous scattering peaks. The crystallinity of PHBV is calculated as the different value between the crystallinity of composites and that of lignin. All results are listed in Table III and the crystallinity of PHBV is placed in parentheses. Although the results are different from those calculated from DSC, the basic trends are the same. As a kind of heterogeneous nucleation agent, lignin powder provided more nucleating sites and increased the crystallinity of composites, as well as that of PHBV. Therefore, the effect of lignin powders on the crystallization process of PHBV can be classified into two aspects, accelerating the nucleation rate while retarding the following crystal growth rate.
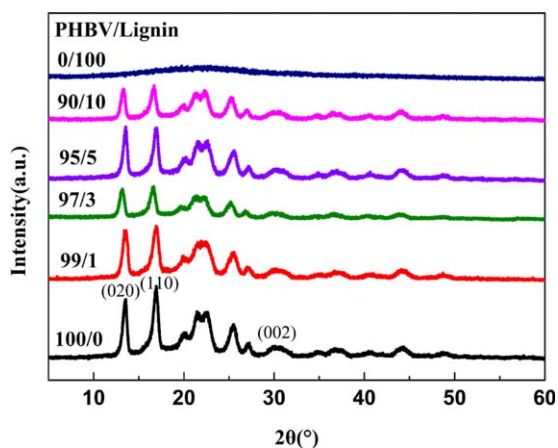

Figure 5. WAXD patterns of PHBV/lignin composites. [Color figure can be viewed in the online issue, which is available at wileyonlinelibrary.com.]

Nucleating Activity and Spherulites Morphology of PHBV/Lignin Composites

To further investigate the nucleation effect of lignin on the spherulites morphology of PHBV, POM was applied to give more detailed information. As shown in Figure 6, without lignin powder, the number of PHBV spherulites was small and the size was relatively big, since the spherulites had large space to grow before impinging on each other [Figure 6(a)]. With the addition of lignin powder, the number of PHBV spherulites increased significantly and consequently their size was dramatically reduced [Figure 6(b)], which was in consistent with the results calculated from WAXD. This phenomenon clearly suggested that the nucleation density of PHBV spherulites was enhanced significantly in the PHBV/lignin composites. The nucleating activity of lignin with respect to the crystallization of PHBV can also be estimated with the method proposed by Dobreva and Gutzowa.[33,34] In the vicinity of the melting temperature (T_{m1}), the cooling rate, and the undercooling (ΔT_p), corresponding to the peak of DSC curve are connected as

$$\text{Lg } Q = A - \frac{B}{2.3\Delta T_P^2} \qquad (7)$$

for the homogeneous case and

$$\text{Lg } Q = A - \frac{B^*}{2.3\Delta T_P^2} \qquad (8)$$

for the heterogeneous nucleation. Where ΔT_P is defined as $T_{m1} - T_P$. B^* is a constant, the ratio B^*/B is defined as the nucleating activity (φ), which is the ratio of the slopes of the linear function LogQ as a function of $1/\Delta T_P^2$ for PHBV/3% lignin and neat PHBV, as represented in Figure 7. The cooling rates were 5°C/min, 10°C/min, 20°C/min, and 40°C/min, respectively. The φ value of 3% lignin in PHBV was about 0.68. The more active the substrate is, the closer φ is to 0; For absolutely inert particles, φ is 1.[35] Therefore, lignin was an effective nucleating agent for PHBV.

The spherulites morphology of PHBV and its composites is shown in Figure 8. PHBV spherulites with characteristic banding and Maltese cross could be seen clearly under POM in Figure 8(a). With the incorporation of lignin powder, the lignin was embedded in the spherulites of PHBV and the integrity of PHBV spherulites was damaged. When the content of lignin

Table III. Data Calculated from WAXD Patterns of PHBV/Lignin Composites

PHBV/Lignin	(hkl)	2θ (°)	d (nm)	F_{WHM}	H_{hkl} (nm)	Crystallinity (%)
100/0	(020)	13.527	0.654	0.553	14.305	59.94 (59.94)
	(110)	16.936	0.523	0.557	14.259	
	(002)	29.852	0.299	1.591	5.110	
99/1	(020)	13.560	0.653	0.645	12.265	61.09 (61.68)
	(110)	16.962	0.522	0.675	11.767	
	(002)	29.850	0.299	1.951	4.167	
97/3	(020)	13.182	0.671	0.622	12.714	66.72 (68.70)
	(110)	16.628	0.533	0.622	12.764	
	(002)	29.714	0.300	1.664	4.884	
95/5	(020)	13.567	0.652	0.516	15.332	63.25 (66.43)
	(110)	16.965	0.522	0.640	12.411	
	(002)	29.975	0.298	1.790	4.543	
90/10	(020)	13.308	0.665	0.563	14.048	66.75 (74.14)
	(110)	16.683	0.531	0.581	13.666	
	(002)	29.752	0.300	1.754	4.634	

was more than 5 wt %, the coalescence phenomenon of lignin was occurred, leading to the appearance of big defects in PHBV spherulites [Figure 8(d,e)]. Besides, sequential images of PHBV spherulites were taken by an attached digital camera every 5 s for measuring of spherulites growth rate. The spherulites radial growth rate was calculated as the slope of the curve of spherulites radius versus growth time. Results are presented as illustrations in Figure 8. With the incorporation of lignin, the interactions between lignin and PHBV became stronger, which decreased the spherulites growth rate of PHBV. As shown in Figure 8(a), the spherulites growth rate of neat PHBV was 3.94 μm s^{-1}, and it decreased to 3.67 μm s^{-1} when added with 1 wt % lignin (Figure 8b). When lignin content was up to 5 wt %, the spherulites growth rate further decreased to 3.23 μm s^{-1} due to the fact that PHBV molecular chains should bypass the conglobated lignin during the crystallization process.

Thermal Stability of PHBV/Lignin Composites
The thermal stability of PHBV/lignin composites was characterized using TGA, and the TG curves are presented in Figure 9.

The initial decomposition temperature T_0, temperature determined at 5% weight loss T_i, maximum decomposition temperature T_{max}, and complete decomposition temperature T_f were obtained from these curves and the values are listed in Table IV. As can be seen from the TG curves, the initial decomposition temperature of PHBV was 254.3°C. Besides, the initial decomposition temperature of PHBV/lignin composites decreased with the increasing content of lignin. When the content of lignin was up to 10 wt %, the initial decomposition temperature of composites decreased to 208.3°C.

Activation energy for decomposition (E_a) of PHBV and its composites can also be calculated from the TG curves by the integral method proposed by Horowitz and Metzger using the equation as follows:[36]

$$\ln\left[\ln\left(\frac{W_0}{W_T}\right)\right] = \frac{E_a\theta}{RT_{max}^2} \qquad (9)$$

where W_0 is the initial weight of polymer, W_T is the residual weight of polymer at temperature T, $\theta = T - T_{max}$ and R is the gas constant. The activation energy is obtained from the slope
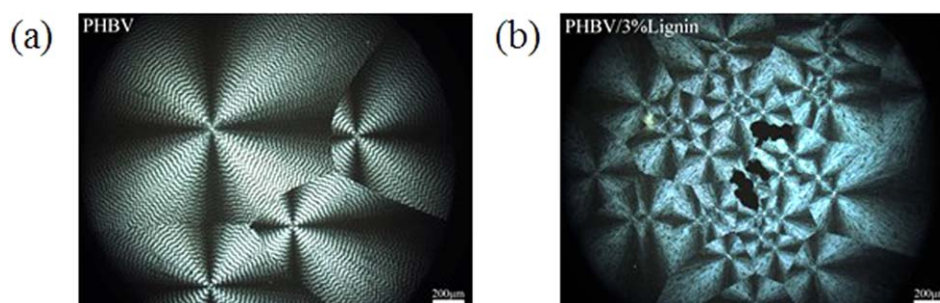

Figure 6. POM images of PHBV (a) and PHBV/3% lignin (b) composites crystallized at 85°C. [Color figure can be viewed in the online issue, which is available at wileyonlinelibrary.com.]
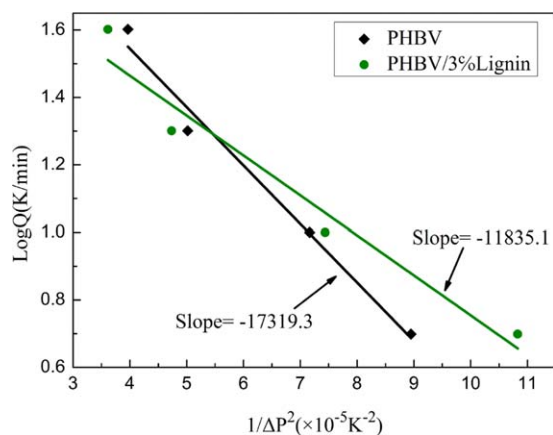
Figure 7. Plot of LogQ versus $1/\Delta T_P^2$ for neat PHBV and PHBV/3% lignin composites. [Color figure can be viewed in the online issue, which is available at wileyonlinelibrary.com.]
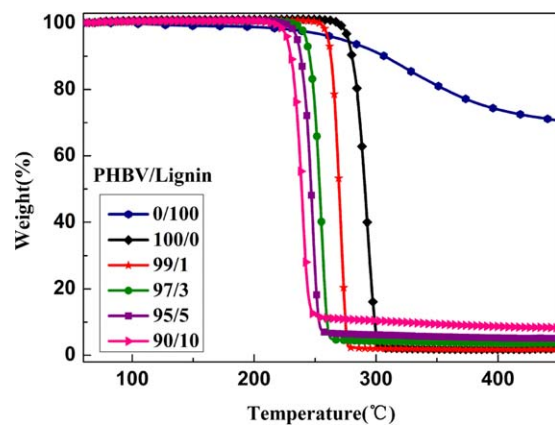

Figure 9. TG curves of PHBV/lignin composites. [Color figure can be viewed in the online issue, which is available at wileyonlinelibrary.com.]

of the plot of $\ln[\ln(W_0/W_T)]$ versus θ for the main stage of thermal degradation (Figure 10) and the values of E_a are listed in Table IV. It is clear that the value of E_a first increased from

431.6 KJ mol^{-1} to 650.1 KJ mol^{-1}, then decreased to 436.7 KJ mol^{-1} with the increasing content of lignin. This phenomenon was the result of double effects of lignin on the PHBV matrix during the degradation process. On the one hand, the existence
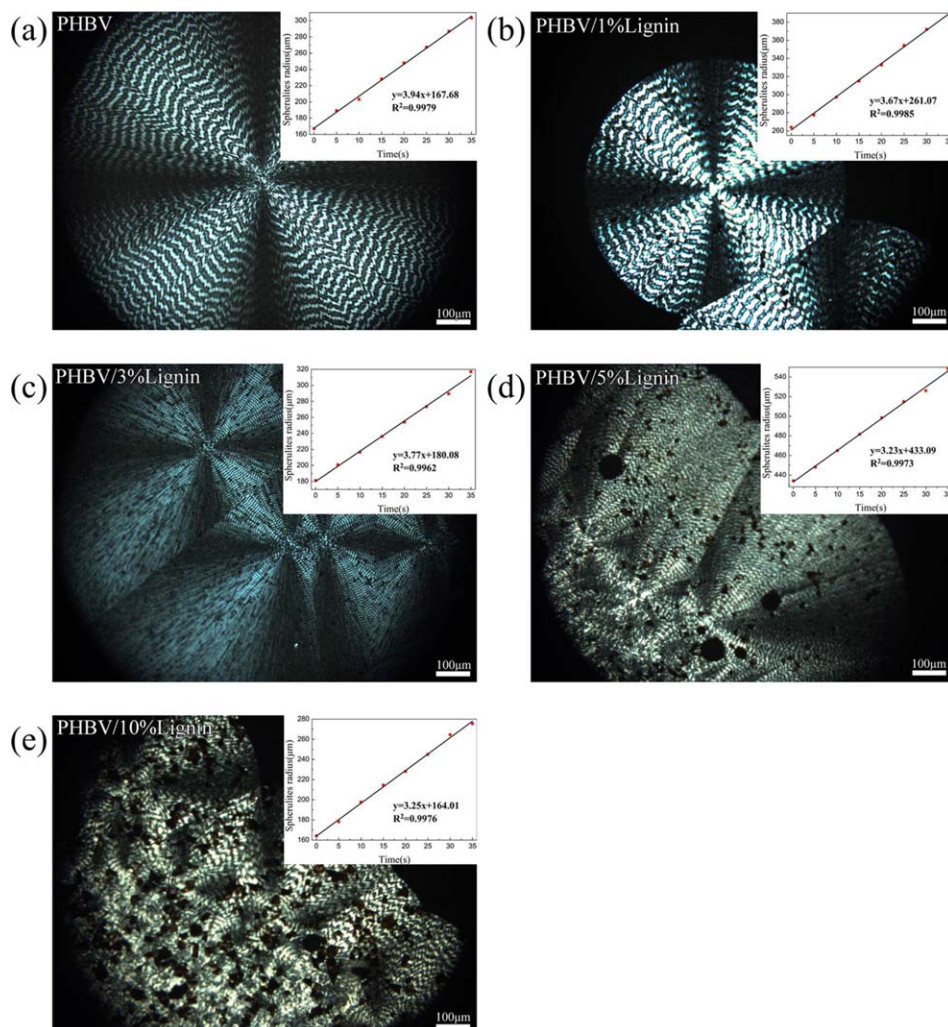

Figure 8. Spherulites morphology and radial growth rate of PHBV/lignin composites [PHBV/lignin: (a) 100/0; (b) 99/1; (c) 97/3; (d) 95/5; (e) 90/10]. [Color figure can be viewed in the online issue, which is available at wileyonlinelibrary.com.]

Table IV. The Thermal Stability Parameters of PHBV/Lignin Composites

PHBV/Lignin	T_0 (°C)	$T_{5\%}$ (°C)	T_{max} (°C)	T_f (°C)	E_a (KJ mol^{-1})
100/0	254.3	277.3	293.2	305.6	431.6
99/1	250.1	260.7	271.2	278.8	650.1
97/3	224.3	242.6	255.5	264.5	502.1
95/5	216.9	235.4	249.0	259.1	471.5
90/10	208.3	227.1	240.6	240.4	436.7
0/100	108.6	272.5	323.5	–	53.1

of hydrogen bonding increased the value of E_a; On the other hand, the E_a value of lignin was very low, only 53.1 KJ mol^{-1}, and the decomposition of –CH$_2$OH groups in lignin accelerated the hydrolysis reaction of PHBV. Therefore, when lignin content was very low, the former effect plays the main role, leading to the increase of E_a. Otherwise, the value of E_a decreased with the addition of lignin.

CONCLUSIONS

The influence of amorphous alkaline lignin on the crystallization behavior and thermal properties of PHBV was investigated in this study. Dual melting peaks caused by the different nucleation mode of PHBV appeared in the DSC curves of PHBV/lignin composites. The effects of lignin on the crystallization process of PHBV can be classified into two opposite way, namely the enhanced effect of nucleation and the hindered effect of spherulites' growth. The addition of lignin did not change the basic crystal structure of PHBV, but damaged the integrity of PHBV spherulites and decreased the average size of the lamellar stacks perpendicular to (020), (110), and (002) lattice planes. In addition, the appearance of lignin also decreased the thermal stability of PHBV.
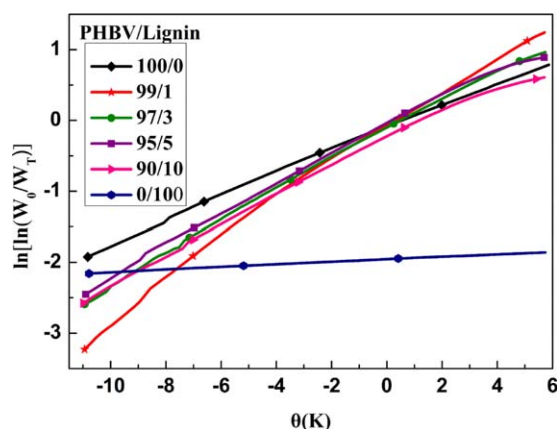

Figure 10. Plots of ln[ln(W_0/W_T)] versus θ for the main stage of thermal degradation of PHBV/lignin composites. [Color figure can be viewed in the online issue, which is available at wileyonlinelibrary.com.]

REFERENCES

1. Khanna, S.; Srivastava, A. K. *Process Biochem.* **2005**, *40*, 607.

2. Liu, Q.; Zhu, M.; Chen, Y. *Polym. Int.* **2010**, *59*, 842.

3. Liu, W. J.; Yang, H. L.; Wang, Z.; Dong, L. S.; Liu, J. J. *J. Appl. Polym. Sci.* **2002**, *86*, 2145.

4. Hobbs, J. K.; McMaster, T. J.; Miles, M. J.; Barham P. J. *Polymer* **1996**, *37*, 3241.

5. Bing-Jie, W.; Yu-Jie, Z.; Jian-Qiang, Z.; Qu-Ting, G.; Zong-Bao, W.; Peng, C.; Qun, G. *Chin. J. Polym. Sci.* **2013**, *31*, 670.

6. Duan, B.; Wang, M.; Zhou, W. Y.; Cheung, W. L. *Polym. Eng. Sci.* **2011**, *51*, 1580.

7. Bittmann, B.; Bouza, R.; Barral, L.; Diez, J.; Ramirez, C. *Polym. Compos.* **2013**, *34*, 1033.

8. Wen, Y.; Chin-Hung, L.; Shao-Jie, W.; Peng-Fei, F.; Yi-Ming, S. *Polymer* **2010**, *51*, 2403.

9. Ten, E.; Turtle, J.; Bahr, D.; Jiang, L.; Wolcott, M. *Polymer* **2010**, *51*, 2652.

10. Yu, H.-Y.; Qin, Z.-Y. *Carbohydr. Polym.* **2014**, *101*, 471.

11. Yu, H.-Y.; Qin, Z.-Y.; Liu, L.; Yang, X.-G.; Zhou, Y.; Yao, J.-M. *Compos. Sci. Technol.* **2013**, *87*, 22.

12. Xiang, H. X.; Chen, S. H.; Cheng, Y. H.; Zhou, Z.; Zhu, M. F. *Express Polym. Lett.* **2013**, *7*, 778.

13. Suttiwijitpukdee, N.; Sato, H.; Zhang, J.; Hashimoto, T.; Ozaki, Y. *Polymer* **2011**, *52*, 461.

14. Wang, S.; Xiang, H.; Wang, R.; Peng, C.; Zhou, Z.; Zhu, M. *Polym. Eng. Sci.* **2014**, *54*, 1113.

15. Jesionowski, T.; Klapiszewski, L.; Milczarek, G. *J. Mater. Sci.* **2014**, *49*, 1376.

16. Sanchez, C. G.; Alvarez, L. A. E. *Angew. Makromol. Chem.* **1999**, *272*, 65.

17. Zhang, R.; Xiao, X.; Tai, Q.; Huang, H.; Hu, Y. *Polym. Eng. Sci.* **2012**, *52*, 2620.

18. Camargo, F. A.; Innocentini-Mei, L. H.; Lemes, A. P.; Moraes, S. G.; Duran, N. *J. Compos. Mater.* **2012**, *46*, 417.

19. Lemes, A. P.; Soto-Oviedo, M. A.; Waldman, W. R.; Innocentini-Mei, L. H.; Duran, N. *J. Polym. Environ.* **2010**, *18*, 250.

20. Wang, S. F.; Song, C. J.; Chen, G. X.; Guo, T. Y.; Liu, J.; Zhang, B. H.; Takeuchi, S. *Polym. Degrad. Stab.* **2005**, *87*, 69.

21. Mousavioun, P.; Doherty, W. O. S.; George, G. *Ind. Crops Prod.* **2010**, *32*, 656.

22. Ma, P. M.; Wang, R. Y.; Wang, S. F.; Zhang, Y.; Zhang, Y. X.; Hristova, D. *J. Appl. Polym. Sci.* **2008**, *108*, 1770.

23. Ahn, B. W.; Chi, Y. S.; Kang, T. J. *J. Appl. Polym. Sci.* **2008**, *110*, 4055.

24. Barham, P. J.; Keller, A.; Otun, E. L.; Holmes, P. A. *J. Mater. Sci.* **1984**, *19*, 2781.

25. Jeziorny, A. *Polymer* **1978**, *19*, 1142.

26. Peng, S. W.; An, Y. X.; Chen, C.; Fei, B.; Zhuang, Y. G.; Dong, L. S. *Eur. Polym. J.* **2003**, *39*, 1475.

27. Barham, P. J. *J. Mater. Sci.* **1984**, *19*, 3826.

28. Wunderlich, B. Macromolecular physics; Academic Press, **1973**, *1*.

29. Shan, G.-F.; Gong, X.; Chen, W.-P.; Chen, L.; Zhu, M.-F. *Colloid Polym. Sci.* **2011**, *289*, 1005.

30. Kunioka, M.; Tamaki, A.; Doi Y. *Macromolecules* **1989**, *22*, 694.

31. Bloembergen, S.; Holden, D. A.; Hamer, G. K.; Bluhm, T. L.; Marchessault, R. H. *Macromolecules* **1986**, *19*, 2865.

32. Botana, A.; Mollo, M.; Eisenberg, P.; Torres Sanchez, R. M. *Appl. Clay. Sci.* **2010**, *47*, 263.

33. Dobreva, A.; Gutzow I. *J. Non-Cryst. Solids* **1993**, *162*, 1.

34. Dobreva, A.; Gutzow, I. *J. Non-Cryst. Solids* **1993**, *162*, 13.

35. Assouline, E.; Lustiger, A.; Barber, A.; Cooper, C.; Klein, E.; Wachtel, E.; Wagner, H. *J. Polym. Sci. Part B: Polym. Phys.* **2003**, *41*, 520.

36. Horowitz, H. H.; Metzger, G. *Anal. Chem.* **1963**, *35*, 1464.